9

Research Article

Xin Yang, Xiang-lin Pei, Jia-jie Xu, Zhi-peng Yang, Wei Gong*, and Jin-cheng Zhong*

Influence of temperature distribution on the foaming quality of foamed polypropylene composites

https://doi.org/10.1515/epoly-2022-8093 received October 23, 2022; accepted December 27, 2022

Abstract: The foamed polypropylene (PP) composites were prepared by injection molding process. Fourier's law and software were used to calculate and simulate the internal temperature distribution of PP composites, respectively, and the influence of the temperature distribution on the foaming quality of foamed PP composites was further analyzed. The result showed that the calculative and simulated results of temperature distribution in different thermal transfer directions had great reproducibility. In different isothermal planes, the temperature from the nozzle to the dynamic mold gradually decreased. The isothermal plane with a temperature of 370.36 K had a better foaming quality, average diameter of cell and cell density were 28.46 μ m and 3.7 \times 10¹⁰ cells·cm⁻³, respectively. In different regions of the same isothermal plane, the temperature gradually decreased from the center to the edge. The foaming quality in the region (c) at a temperature of 335.86 K was ideal, and the average diameter of cell and the cell density were 26.5 μ m and 2.39 \times 10¹⁰ cells·cm⁻³, respectively. This work could provide prediction for improving the foaming quality of foamed polyolefin composites.

Keywords: temperature field, polypropylene, foaming quality, simulation, calculation

Xin Yang, Xiang-lin Pei: School of Materials and Architectural Engineering, Guizhou Normal University, Guiyang 550025, China Jia-jie Xu, Zhi-peng Yang: School of Mechanical and Electrical Engineering, Guizhou Normal University, Guiyang 550025, China

1 Introduction

Nowadays, the foamed polyolefin composites (1,2) have attracted increasing attention due to their excellent comprehensive properties. Compared with traditional polyolefin composites, the foamed polyolefin composites possess specific properties, including good thermal stability, excellent sound absorption property, low thermal conductivity and dielectric constant, etc. (2,3). Thus, foamed polyolefin composites have been widely used in transportation, military industry, aerospace, electronics, daily necessities, and so on (4). Injection molding process is an effective method for massive production of foamed polyolefin composites (5) and has been considered as one of the most common method for foamed polyolefin composites (6,7). Compared with general foaming materials (8,9), foamed PP composites has an ideal environment friendly foam material. However, there will be thermal loss in the injection molding process, which will lead to the change in foaming quality of foamed PP composites. Therefore, it has become a new research direction to explore the influence of temperature distribution on the foaming quality of foamed PP composites.

Recently, more and more researchers have focused on the research of foamed PP composites. Yeh et al. (10) studied the effect of mold temperature on the structure of cells for PP/rice husk natural fiber composites. The result showed that with the decrease in the mold temperature, the cell density decreased more significantly. Wang et al. (5) studied the influence of different barrel temperatures on the properties of foamed PP components. They found that the sample weight and cell density decreased with increase in the barrel temperature. Chung et al. (11) used semi-crystalline PP and polystyrene (PS) as matrix materials, then studied the effects of melting temperature and mold temperature on the weight, specific gravity, and expansionary rate of samples. The result showed that semi-crystalline PP exhibited the highest expansionary rate at high melting temperature and low mold temperature, while PS exhibited the highest

^{*} Corresponding author: Wei Gong, School of Materials and Architectural Engineering, Guizhou Normal University, Guiyang 550025, China; National Engineering Research Center for Compounding and Modification of Polymer Materials, Guiyang 550025, China; School of Mechanical and Electrical Engineering, Guizhou Normal University, Guiyang 550025, China,

e-mail: gw20030501@163.com

^{*} Corresponding author: Jin-cheng Zhong, School of Materials and Architectural Engineering, Guizhou Normal University, Guiyang 550025, China, e-mail: zhongjc16@163.com

expansionary rate at medium melting temperature and low mold temperature. Liu et al. (12) studied the effect of foaming temperature on the cell structure of ultra-high molecular weight polyethylene and supercritical carbon dioxide by foaming process. The result showed that the cell size and cell density were affected by crystal structure, temperature, and higher foaming temperature leaded to larger cell size and lower cell density. Nakano and Shimbo (13) used a device that allows precise control of temperature and pressure to obtain samples and discussed the relationship between the cell density, foaming time, and foaming temperature. The result showed that the cell density of foamed PS and polycarbonate (PC) composites became larger at lowtemperature. The effects of foaming temperature and mold temperature on the foaming quality of foamed PP composites had been investigated, and some significant theoretical results had been obtained. However, there were few studies on the effect of internal temperature distribution on the foaming quality of foamed PP composites.

In this study, we investigated the injection molding process of foamed PP composites using Fourier's law and simulation calculations. The effect of the variation in the temperature field in different regions of the material on the structure of the vesicles in each micro-region was investigated. This provides a reference for the development of foamed PP composites with different cell structures.

2 Materials and methods

2.1 Materials

PP T-30s was supplied by Anhui Fengyuan Co., Ltd, with the melt mass flow rate (MFR) of 3.2 g per 10 min. Low-density polyethylene (LDPE) 2426H was supplied by Lanzhou Petrochemical Co., with the MFR of 1.8 g per 10 min. Azodicarbonamide (AC) was gained from Shenzhen Jiaxinhao Plastic Products Co., Ltd. Zinc stearate [Zn(St)₂] was supplied by Wenzhou Jia Da Plastic Additives Co., Ltd. Zinc oxide (ZnO) was supplied by Xiangyun County Hongxiang Co., Ltd. Montmorillonite (MMT) was supplied by Wuhan Hanhong Chemical Plant.

2.2 Sample preparation

2.2.1 Preparation of PP/MMT blend

The PP and MMT were dried at 60°C for 8 h before processing. MMT was added to PP at 3 wt% on a twin-screw

extruder (CTE20, Coperion Koryo Nanjing Machinery Co., Ltd, Nanjing, China) for obtaining the masterbatch, and the parameters of the extrusion process were as follows: temperature of 175–185°C, screw speed of 100 rpm, feeding speed of and 10 rpm.

2.2.2 Preparation of foaming agent masterbatch

AC and LDPE were dried at 60°C for 4 h before the process. Afterwards, they were blended in a torque rheometer (XSS-300, Shanghai Kechuang Rubber & Plastic Machinery Equipment Co., Ltd), with a LDPE/AC weight ratio of 90/10 (14). The temperature was set to 110°C.

2.2.3 Preparation of foaming auxiliary masterbatch

ZnO and Zn(St)₂ were dried at 60°C for 4 h before processing. ZnO and Zn(St)₂ were evenly mixed at a mass fraction ratio of 5:1, then added to 94 parts of PP and evenly mixed (15). The foaming auxiliary masterbatch was prepared by twin screw extrude (CTE20, Coperion Koryo Nanjing Machinery Co., Ltd, Nanjing, China). The temperature of each section of the extrude from hopper to the nozzle was set from 175°C to 185°C. The screw rotation speed was 100 rpm and the feeding speed was 10 rpm.

2.2.4 Preparation of foam

The PP/MMT blend was dried at 80°C for 8 h. Then, the PP matrix, the foaming masterbatch and the foaming auxiliary masterbatch were uniformly mixed at 85:10:5 mass fraction ration (16). The foamed samples were prepared by the injection molding machine (EM120-V, Zhende plastic machinery Co., Ltd) and the temperature from hopper to nozzle was set from 165°C to 190°C. The technique parameters are shown in Table 1.

2.2.5 Slice of samples

First, the foamed sample was obtained by injection molding, The thickness of foamed spline is larger than that of unfoamed spline, and the thickness difference is 0.5 mm. Uniform slicing were made along the thickness direction of the foamed sample (Figure 1a). Then, the different isothermal planes of the samples (Figure 1b) and different regions of the same isothermal plane (Figure 1c) were obtained with a self-made cutter.

Table 1: Foamed polypropylene composites injection molding technique parameters

Injection pressure (bar)	Mold temperature (°C)	Melting temperature (°C)	Injection speed (%)	Cooling time (s ⁻¹)
50	35.6	190	95	30

According to the order of slices, the different isothermal planes of the sample were set as follows: melting plane (S-0), isothermal plane (S-1), isothermal plane (S-2), isothermal plane (S-3), isothermal plane (S-4), and dynamite mold plane (S-5), and the temperatures were set as t_0 , t_1 , t_2 , t_3 , t_4 , and t_5 , respectively.

For different regions of the same isothermal plane, region (a), region (b), region (c), and region (d), and their respective symmetrical regions, region (b'), region (c'), and region (d') were set. The temperatures set were $t_{\rm a}$, $t_{\rm b}$, $t_{\rm c}$, $t_{\rm d}$, $t_{\rm b'}$, $t_{\rm c'}$, and $t_{\rm d'}$, respectively. Since $t_{\rm b} = t_{\rm b}$, $t_{\rm c'} = t_{\rm c'}$, and $t_{\rm d} = t_{\rm d'}$, region (a), region (b), region (c), and region (d) were investigated.

2.3 Characterization

2.3.1 Scanning electron microscopy (SEM)

SEM (TM-4000Plus, Hitachi Scientific Instruments Co. Japan) was used to observe the morphology of the samples. Take the cut sample on the conductive adhesive, spray gold for 40 s, give the material conductivity, and then place the sample in the SEM for surface morphology

test. The average size and distribution of cell size in the samples were analyzed with Nano-Measure software (Media Cybernetic, Rockville, MD, USA), and the distribution of cell size could be denoted with a distribution coefficient (S_d), as shown by Eqs. 1–4 (17,18).

$$V_{\rm f} = 1 - \frac{\rho_{\rm f}}{\rho} \tag{1}$$

$$\bar{D} = \frac{1}{n} \sum_{i=1}^{n} D_i \tag{2}$$

$$N_{\rm c} = \left(\frac{n}{A}\right)^{\frac{3}{2}} \times \left(\frac{1}{1 - V_{\rm f}}\right) \tag{3}$$

$$S_{\rm d} = \sqrt{\sum_{1}^{n} (D_i - D)^2 \frac{1}{n}}$$
 (4)

where n is the number of cells in the SEM image, D_i is the diameter of a single cell (μ m), \bar{D} is the average diameter of cells (μ m), V_f is the foaming ratio (%), A is the area of the image (cm²), ρ_f is the foamed materials' density (g·cm³), ρ is the unfoamed materials' density (g·cm³), and S_d is the distribution coefficient of cells (μ m). The ρ_f and ρ were measured with an electronic densimeter (JM300, Nanjing Technology Co., Ltd).

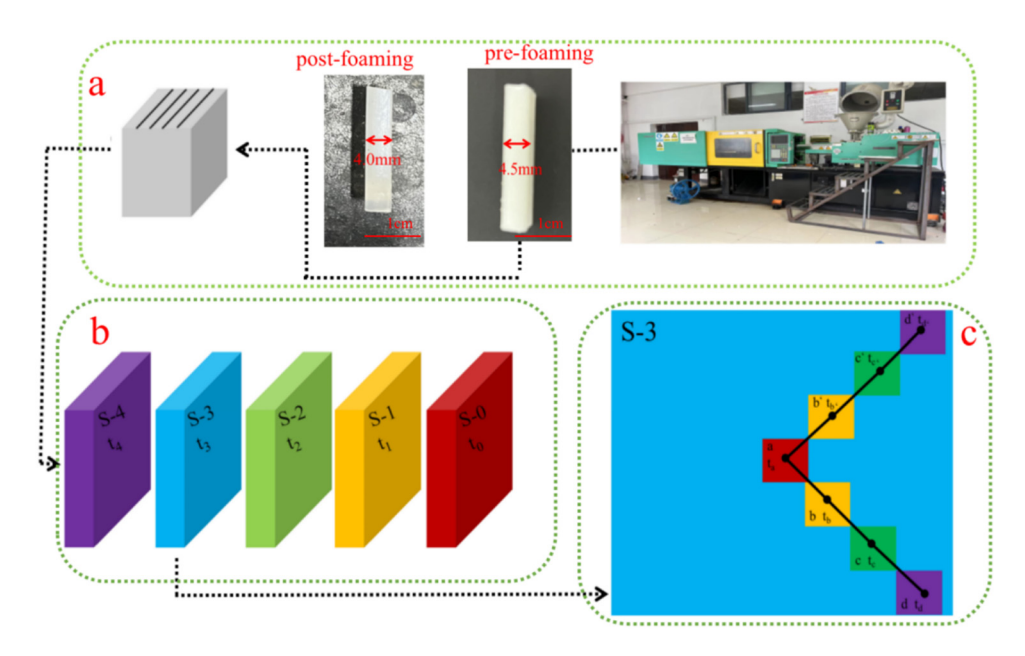


Figure 1: Schematic diagram of slices (a), different isothermal planes (b), and (c) different regions of the same isothermal plane.

3 Results and discussion

3.1 Calculation and simulation of temperature distribution

3.1.1 Calculation of temperature distribution

According to the Fourier's law (19), for a uniformly textured object, the thermal energy per unit time, Q, was proportional to the temperature gradient, and the thermal transfer area, A, was perpendicular to the direction of thermal flow, as shown in Eqs. 5–7.

$$Q = -\lambda A \frac{\mathrm{d}t}{\mathrm{d}x} \tag{5}$$

$$q = \frac{Q}{A} \tag{6}$$

$$\int_{t_0}^{t_5} \mathrm{d}t = -\frac{Q}{\lambda A} \int_0^b \mathrm{d}x \tag{7}$$

where Q is the thermal energy (W); q is the heat flux (W·m⁻²); $\frac{dt}{dx}$ is the thermal conductivity of samples (W·m⁻¹·K⁻¹); $\frac{dt}{dx}$ is the temperature gradient in the X direction, which is the direction of temperature reduction (Figure 2); t_0 is the mold temperature (K); and t_5 is the melting temperature (K). Assuming that the material is homogeneous, the thermal conductivity value is a constant in the process. The temperature on both sides of the sample is known, that is, x = 0, $t = t_0$; x = b, and $t = t_5$. It is known that the thermal conductivity is 0.22 W·m⁻¹·K⁻¹ (20). The melting temperature t_0 is 463 K, and the mold temperature t_5 is 308.6 K. The

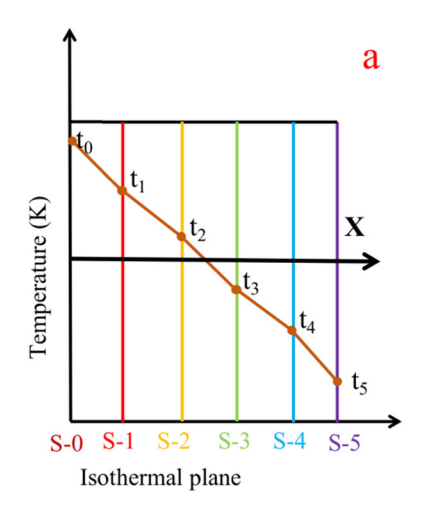
thermal transfer distance b_1 from S-0 to S-5 is 4.5 mm (Figure 3a), and the thermal transfer distance b_2 from the center to edge is 5 mm (Figure 3b).

Using the above Eqs. 5 and 6, the thermal fluxes $q_1 = 7,548.5 \text{ W}\cdot\text{m}^{-2}$ and $q_2 = 2,728 \text{ W}\cdot\text{m}^{-2}$ could be calculated, respectively, and the temperature values of the different isothermal planes and the different regions of the same isothermal plane could be calculated by Eq. 7, as shown in Figure 4.

Figure 4 showed the calculative values of temperature distribution for PP composites. It could be seen that the temperature of isothermal plane from nozzle to dynamic mold plane gradually decreased from 432.12 to 339.48 K (Figure 4a). The main reason for this phenomenon was that the thermal loss between the nozzle and dynamic mold plane gradually increased during the injecting molding process, which led to the gradual decrease in temperature. According to Figure 4b, it could be seen that the calculative values of temperature distribution from the center to edge gradually decreased on the isothermal plane (S-3), and the temperature in the central region (a) was the highest with a value of 370.36 K. The temperature in region (b) was 389 K, in region (c) was 335.86 K, and in region (d) was 318.3 K. This was mainly due to the thermal transfer from high temperature to low temperature.

3.1.2 Simulation of temperature distribution

The solid thermal transfer interface in the software was used to simulate PP composites (21,22). The cubic model (Figure 5a) was established with the size of $10 \text{ mm} \times 10 \text{ mm} \times 4.5 \text{ mm}$, and the plane model with the



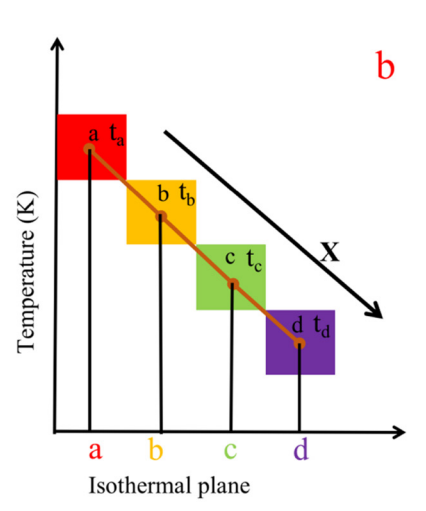


Figure 2: Schematic diagram of thermal transfer direction of PP composites: (a) different isothermal planes and (b) different regions of the same isothermal plane.

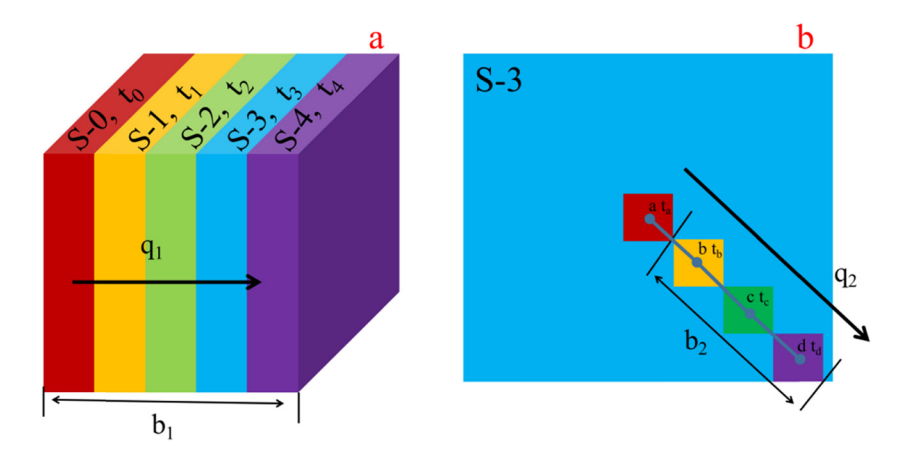


Figure 3: Schematic diagram of the parameters of PP composites: (a) different isothermal planes and (b) different regions of the same isothermal plane.

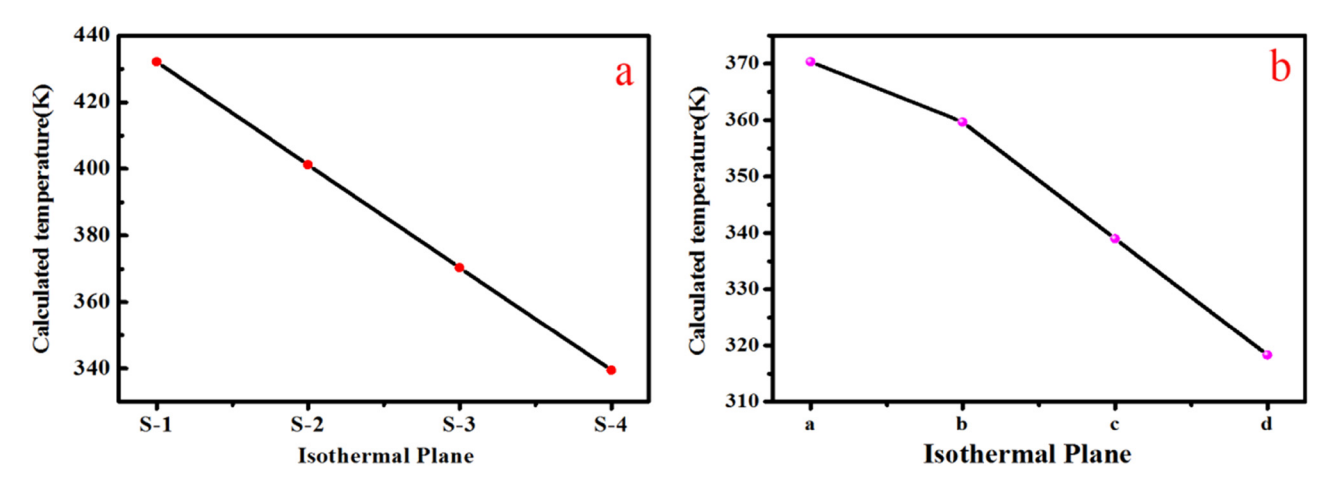


Figure 4: Calculation of the thermal transfer direction inside the foamed PP composites: (a) different isothermal planes and (b) different regions of the same isothermal plane.

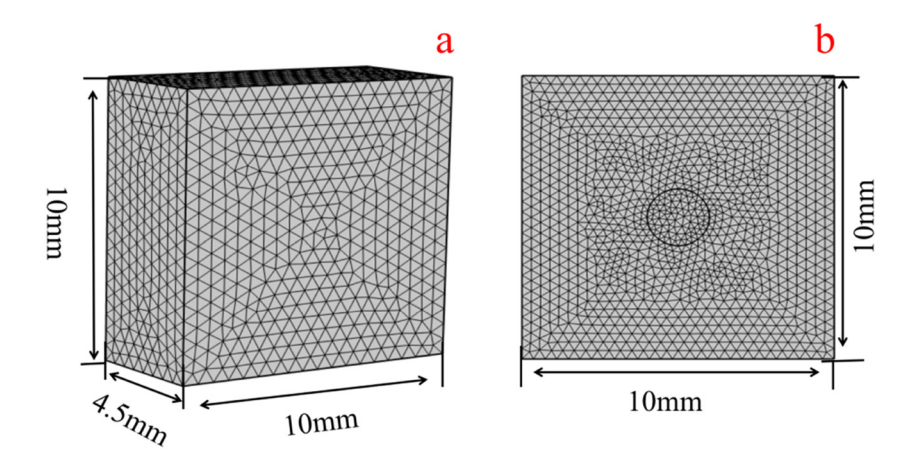


Figure 5: Schematic diagram of the size of the simulation model of PP composites: (a) cubic model and (b) plane model.

size of 10 mm \times 10 mm, respectively (Figure 5b). The thermal conductivity was 0.22 W·m⁻¹·K⁻¹ (23), the constant pressure thermal capacity was 1,900 J·kg⁻¹·K⁻¹ (24), and the thermal transfer parameter was 1,225 W·m⁻²·K⁻¹ (25).

Figures 6 and 8a show the trends of simulation temperature and specific simulation values of different isothermal planes, respectively. From isothermal planes of S-1 to S-4, the simulated temperature gradually decreased

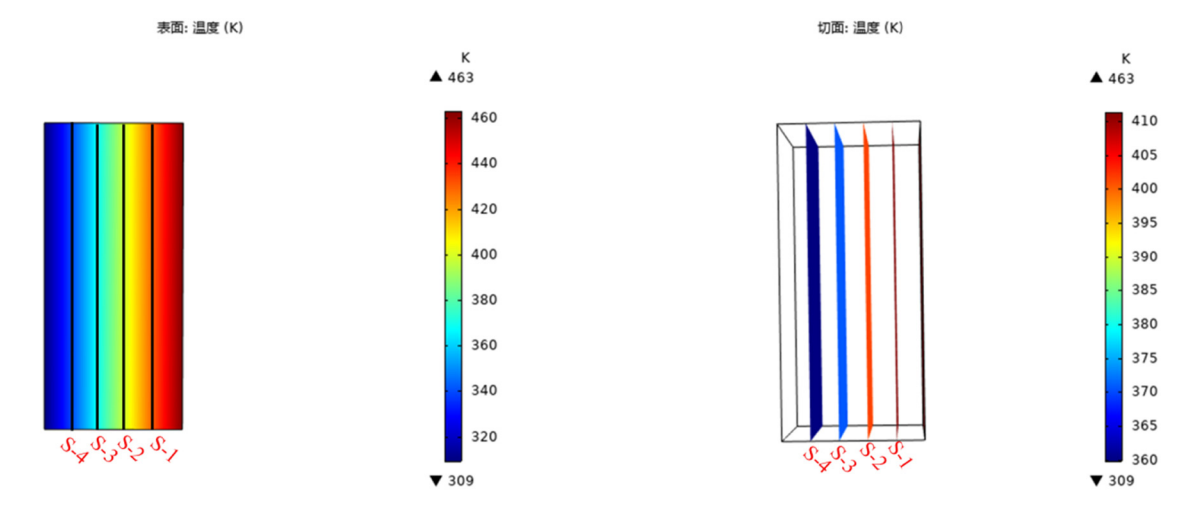


Figure 6: Simulation temperature results of different isothermal planes of PP composites.

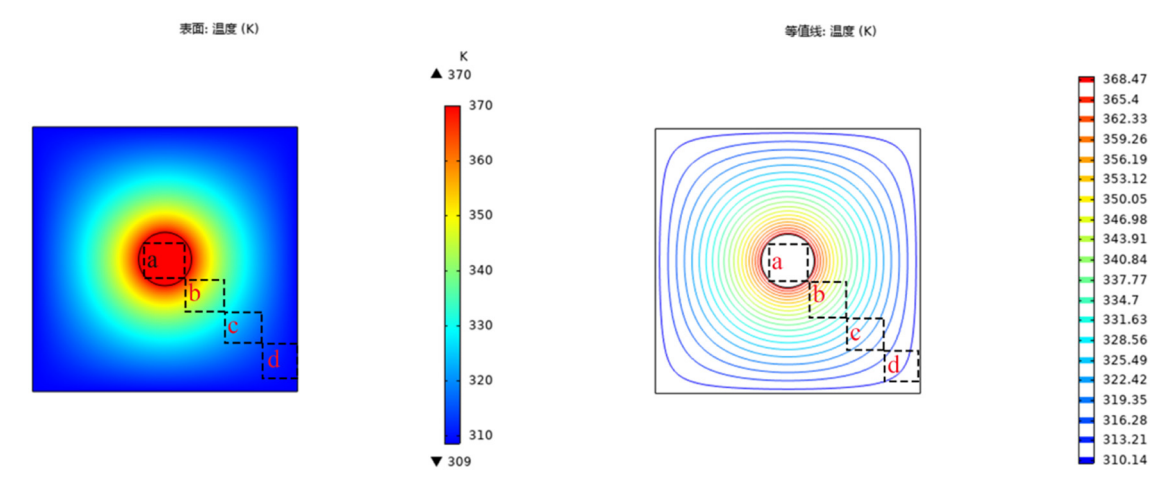


Figure 7: Schematic of software simulation of the thermal transfer from the center to the edge on the same plane.

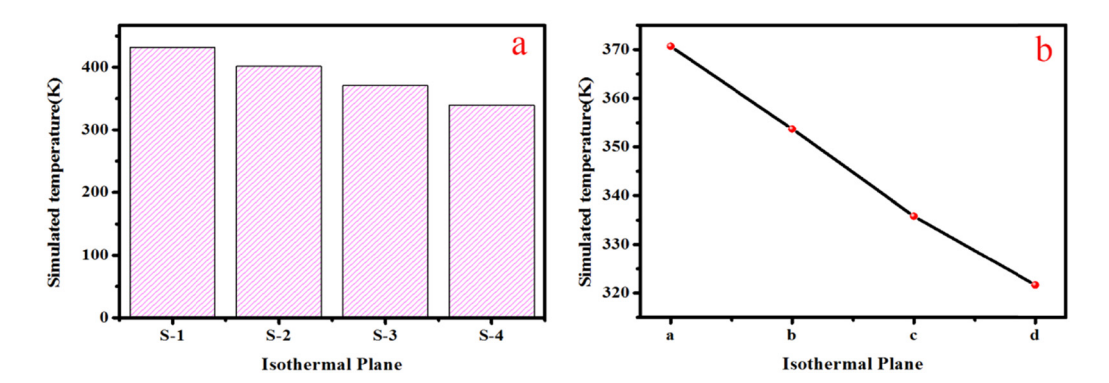


Figure 8: Simulation of the thermal transfer direction inside the PP: (a) different isothermal planes and (b) different regions of the same isothermal plane.

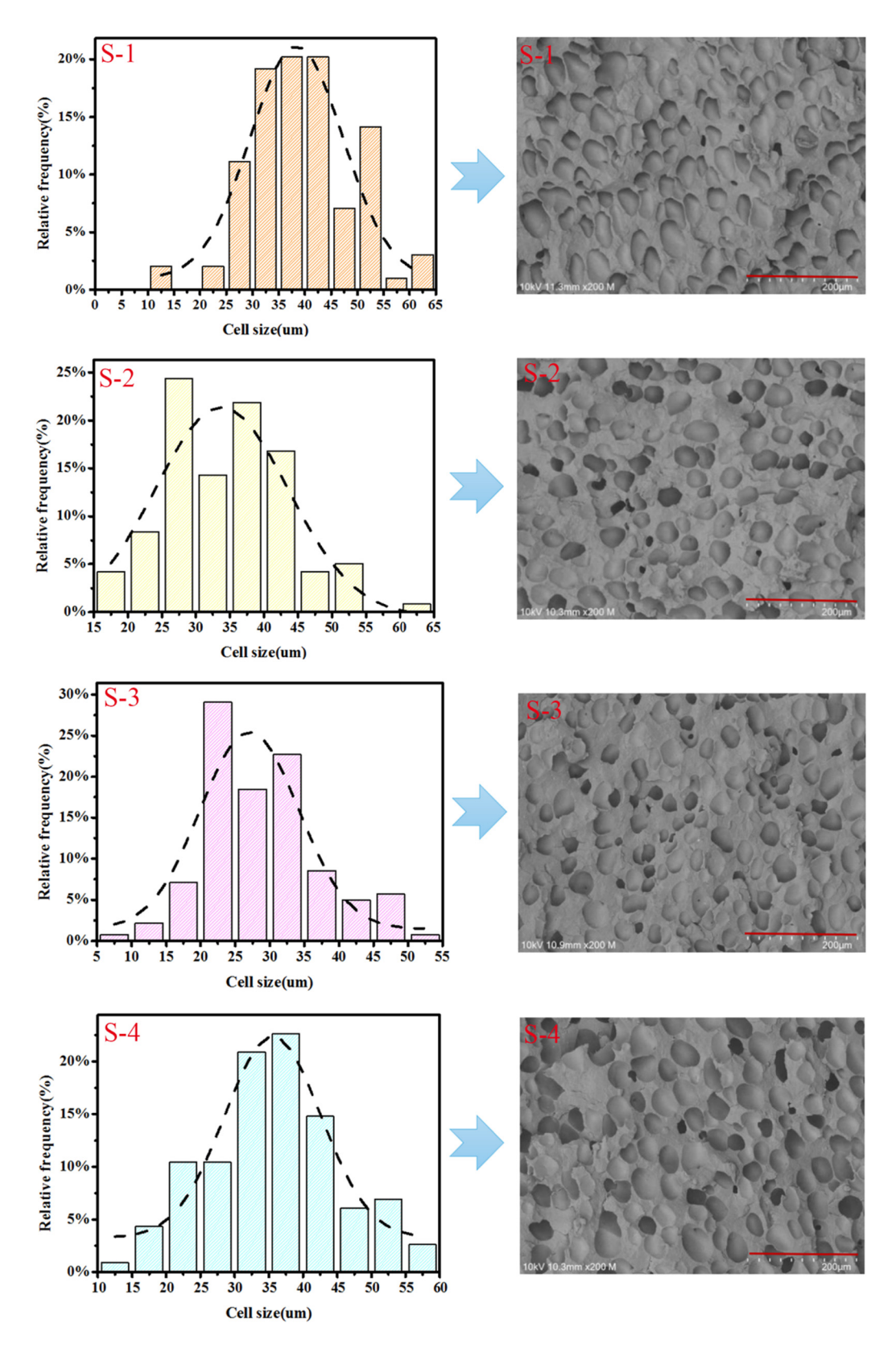


Figure 9: Foaming quality of foamed PP composites in different planes.

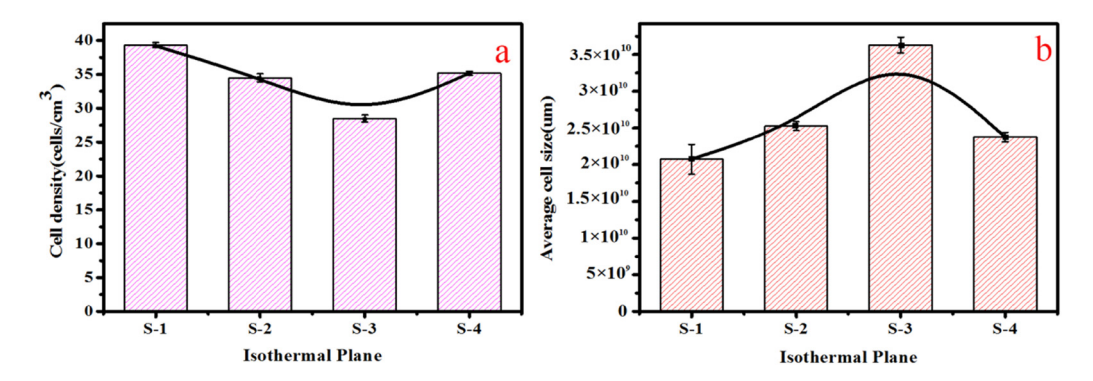


Figure 10: Parameters of the cell structure of different planes of PP foamed composites: (a) cell density and (b) average cell diameter.

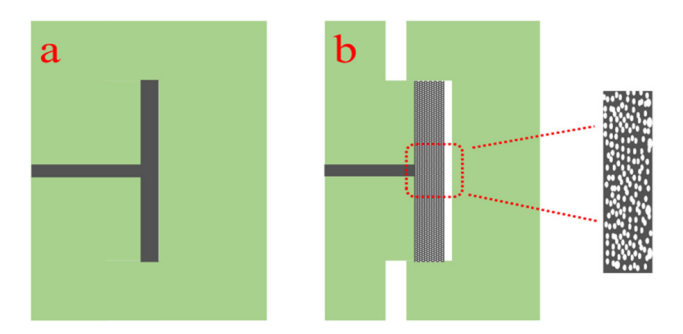


Figure 11: The schematic of the foaming process with adjustable volume: (a) injection process and (b) open mold.

from 432.12 to 339.91 K (Figures 6 and 8a). Figure 7 shows the trends of simulated temperature in different regions of the same isothermal plane. It could be seen that the simulated temperature in central region (a) was the highest with a value of 370.68 K, and gradually decreased from the central region to other regions. The simulated temperature in region (d) was the lowest with a value of 321.66 K (Figures 7 and 8b). The simulated results were consistent with the calculative

results in Section 2.1.1. The calculated and simulated results provide a basis for improving the foaming quality of foamed PP composites.

3.2 Effect of temperature distribution on foaming quality of foamed PP composites

3.2.1 Effect of foaming quality of foamed PP composites on different isothermal planes

Figure 9 shows the cell distribution and cell morphology of the foamed PP composites in different isothermal planes. It could be seen that the cell size of S-1, S-2, S-3, and S-4 were mainly concentrated among 30–45, 25–30, 25–30, and 30–40 μ m, respectively. The cell diameter of S-3 was relatively concentrated and evenly distributed. Figure 10 shows the cell structure parameters of foamed PP composites with different isothermal planes. From isothermal planes of S-1

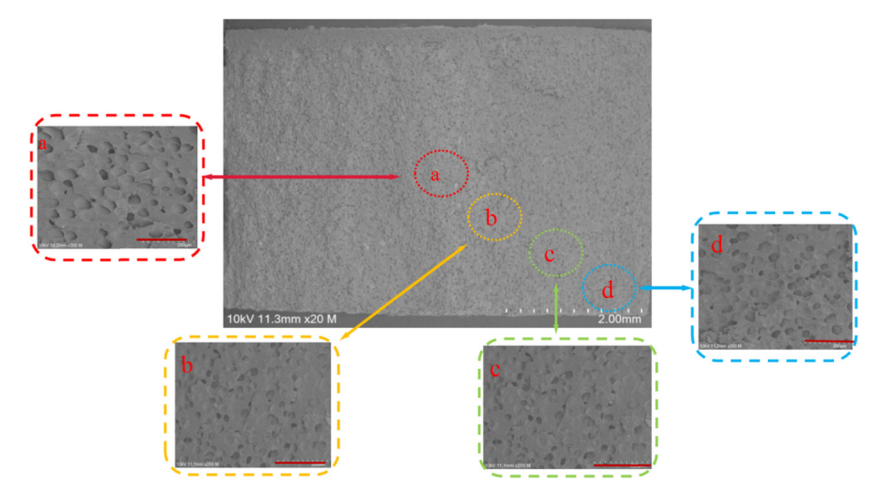


Figure 12: Structure of cells in different regions of the same isothermal plane.

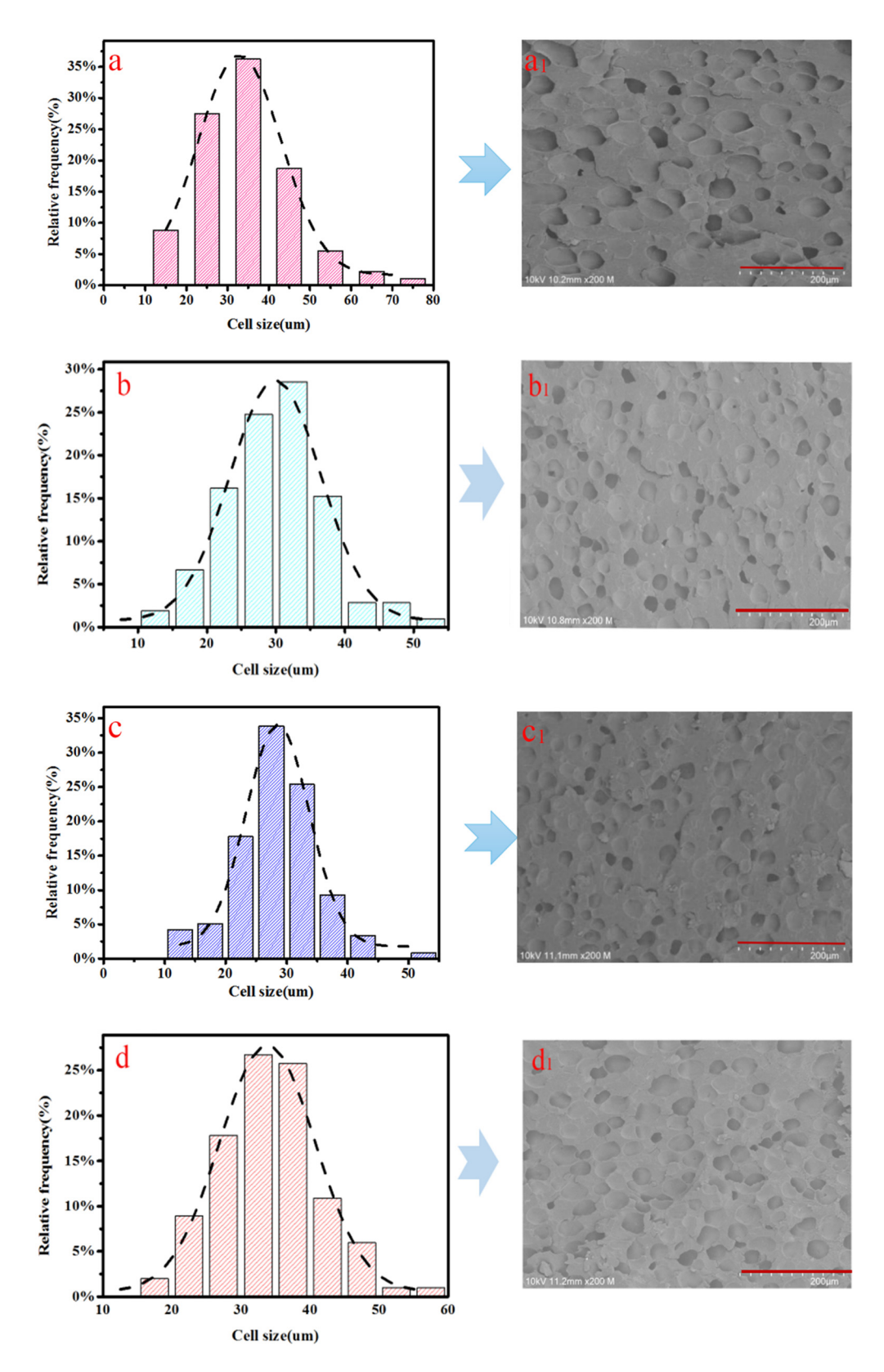
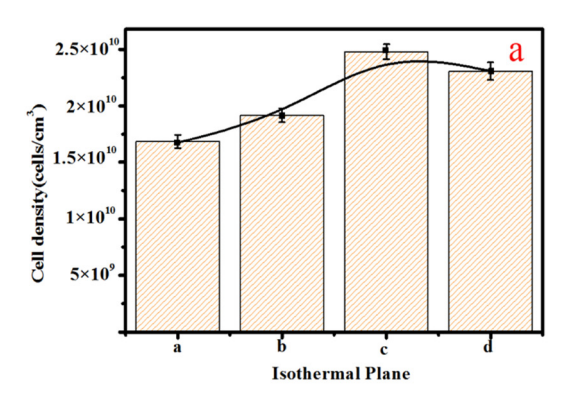


Figure 13: Quality of cells in different regions of the same isothermal plane for foamed PP composites: (a-d) distribution of cells at various regions and (a_1-d_1) electron micrographs of cells in different regions.



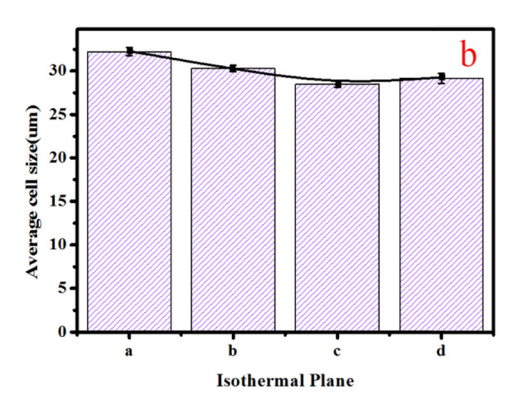


Figure 14: Structural parameters of the cells in different regions of the same isothermal plane for the PP foam: (a) cells density and (b) average cell diameter.

to S-4, the cell size first decreased and then increased, while the cell density first increased and then decreased (Figure 10a and b). According to the result of calculation and simulation, the temperature decreased gradually from the isothermal planes of S-1 to S-4, and increased the polymer melt viscosity, strength of melt, strengthened the ability to hinder cell growth and reduced the cell growth, and made the average cell diameter smaller and the cell density larger. However, the average diameter of cells increased gradually from S-3 to S-4, and the cell density decreased with the increase in cell size. The main reason was that few cells would be produced at the nozzle during injection molding process, and when the resin was ejected from the nozzle, the formed cells deformed due to the migration of resin (26). For different isothermal planes, when the melt touched the mold (Figure 11), the surface tension of the cells did not drag the stretched cells back into a circle and the cells cooled and shaped rapidly (27,28). It could be observed that the cell size of the isothermal plane (S-4) was larger.

3.2.2 Effect of foaming quality of foamed PP composites on different regions of the same isothermal plane

From the influence of temperature distribution of different isothermal planes on the foamed PP composites, it could be seen that the foaming quality on the isothermal plane at 370.36 K was ideal. Therefore, the influence of foaming quality of foamed PP composites on different regions of the same isothermal plane is explored, and the results are shown in Figures 12–14.

Figures 12 and 13 show the cell distribution diagram and cell morphology diagram of different regions of the same isothermal plane for foamed PP materials. It could be seen that the cells' size in region (a) were mainly concentrated among 30–40 µm, in region (b) among 25–35 µm,

in region (c) among 25-30 µm, and in region (d) among 30-35 µm, and the cells' diameter in region (c) were relatively smaller and the cells uniformity were relatively greater. Figure 14 shows the parameters of cell structure for the foamed PP composites in different regions of the same isothermal plane. On the same isothermal plane, the cell density first increased and then decreased, while the cell size first decreased and then increased. The foaming quality in region (a) was poor, and the average cell diameter and cell density were 31.5 μ m and 1.6 \times 10¹⁰ cells·cm⁻³, respectively. The foaming quality in region (c) was better, and the average cell diameter and cell density were 26.5 µm and 2.39×10^{10} cells·cm⁻³, respectively. According to the results of calculation and simulation, the temperature decreased gradually from different regions of the same isothermal plane from region (a) to region (d), and increased the polymer melt viscosity, melt strength, strengthened the ability to hinder cell growth and reduced the cell growth, and made the average cell diameter smaller and the cell density larger (28,29). At the same time, in the injection molding process, the cells from the nozzle were deformed due to the migration of the resin. For different regions of the same iso-thermal plane, when the melt contact with both sides of the mold (Figure 11), then the cells cooled rapidly so that the surface tension of the cells did not drag the stretched and deformed cells back to the round (27-30). It could be observed that the cell size in the region (d) was larger.

4 Conclusion

1. Fourier's law and software were used to calculate and simulate the internal temperature distribution of PP composites, the temperature gradually decreased from nozzle (S-0) to dynamic mold plane (S-5) in different isothermal planes, that is, from 463 to 308.6 K. On

- the same isothermal plane, the calculative temperature decreased gradually from the center to the edge of the isothermal plane, and the temperature in the center region (a) was the highest with a value of 370.36 K.
- 2. Software simulation showed that the simulated temperature decreased gradually from S-1 to S-4 isothermal plane, from 432.12 to 339.91 K. For different regions of the same isothermal plane, the simulated temperature decreased gradually from the central region to other regions. The simulated temperature in the central region (a) was the highest with a value of 370.68 K, and the simulated temperature in the central region (d) was the lowest with a value of 321.66 K. The simulated results were consistent with the calculated results.
- 3. Among the different isothermal planes, the isothermal plane with a temperature of 370.36 K (S-3) had a better foaming quality, the average cell diameter and cell density were 28.46 μ m and 3.7 \times 10¹⁰ cells·cm⁻³, respectively. In different regions of the isothermal plane at 335.86 K, the foaming quality in region (c) was more desirable, the average cell diameter and cell density were 26.5 μ m and 2.39 \times 10¹⁰ cells·cm⁻³, respectively.

Acknowledgments: I would like to express my gratitude to all those who helped me during the writing of this thesis. I sincerely thank my teacher Professor Gong for his help and financial support. In addition, I would like to thank Guizhou Normal University for providing a learning platform. Finally, I would like to thank the editors of e-polymers for their help.

Funding information: This work was supported by the National Natural Science Foundation of China (No. 52063008), the Natural Science Foundation Funding Projects of Guizhou Province (No. ZK [2021]050), the Foundation of Guizhou Scientific Research Institute (QianKeFuQi [2018] 4010), and the Hundred Talents Project of Guizhou Province (No. [2016]5673).

Author contributions: Xin Yang and Wei Gong: designed and performed the experiments; Xin Yang, Jia-Jie Xu, and Zhi-peng Yang: data curation and formal analysis; Xin Yang: writing - original draft; Xiang-lin Pei and Jincheng Zhong: writing - review and editing; Wei Gong: funding acquisition. All authors have read and agreed to the published version of the manuscript.

Conflict of interest: Authors state no conflict of interest.

Data availability statement: The data presented in this study are available on request from the corresponding author.

References

- Gong W, Fu H, Zhang C, Ban D, He Y, Pei XL, et al. Study on foaming quality and impact property of foamed polypropylene composites. Polym. 2018;10(12):1375-86. doi: 10.3390/ polym10121375.
- Li M, Huang T, Qin Y, Shen C, Gao S. Preparation process orthogonal optimization and mechanical properties of microcellular foam polypropylene. Macromol Mater Eng. 2021;306(10):2100350-61. doi: 10.1002/mame.202100350.
- Liu B, Jiang T, Zeng X, Deng R, Gu J, Gong W, et al. (3) Polypropylene/thermoplastic polyester elastomer blend: crystallization properties, rheological behavior, and foaming performance. Polym Advan Technol. 2021;32(5):2102-17. doi: 10.1002/pat.5240.
- (4) Hamidinejad M, Zhao B, Zandieh A, Moghimian N, Filleter T, Park B. Enhanced electrical and electromagnetic interference shielding properties of polymer-graphene nanoplatelet composites fabricated via supercritical-fluid treatment and physical foaming. ACS Appl Mater Inter. 2018;10(36):30752-61. doi: 10.1021/acsami.8b03777.
- Wang J, Mao Q, Jiang N. Effects of injection molding parameters on properties of insert-injection molded polypropylene single-polymer composites. Polym. 2021;14(1):23-33. doi: 10.3390/polym14010023.
- Gong W, Wang DJ, Jiang TH, Zeng X, Zhang C, He L. Cell growth, deformation and model establishment of micro-foamed polystyrene material. J Mater Res Technol. 2021;13:2260-71. doi: 10.1016/j.jmrt.2021.05.077.
- Ren J, Lin L, Jiang J, Li Q, Hwang SS. Effect of gas counter pressure on the surface roughness, morphology, and tensile strength between microcellular and conventional injectionmolded PP parts. Polym. 2022;14(6):1078-89. doi: 10.3390/ polym14061078.
- Albuquerque RQ, Brütting C, Standau T. A machine learning investigation of low-density polylactide batch foams. Epoly. 2022;22(1):318-31. doi: 10.1515/epoly-2022-0031.
- Yang K, Gong P, Yang L. The effect of different structural designs on impact resistance to carbon fiber foam sandwich structures. Epoly. 2022;22(1):12-8. doi: 10.1515/epoly-2022-0003.
- (10) Yeh SK, Yang SH, Han L, Liu HY, Liao YS, Chang YC. Foam extrusion of polypropylene-rice husk composites using CO2 as the blowing agent. J Cell Plast. 2019;55(4):401-19. doi: 10.1177/0021955X19839744.
- Chung CY, Hwang SS, Chen SC, Lai MC. Effects of injection (11)molding process parameters on the chemical foaming behavior of polypropylene and polystyrene. Polym. 2021;13(14):2331-45. doi: 10.3390/polym13142331.
- Liu J, Qin S, Wang G, Wang G, Zhang H, Zhou H, et al. Batch foaming of ultra-high molecular weight polyethylene with supercritical carbon dioxide: Influence of temperature and pressure. Polym Test. 2021;93:106974-86. doi: 10.1016/j. polymertesting.2020.106974.
- (13)Nakano S, Shimbo M. Experiments on solid-state cell nucleation in polystyrene and polycarbonate as a function of foaming temperature and foaming time. Cell Polym. 2006;25(3):127-42. doi: 10.1177/026248930602500301.
- Xi Z, Chen J, Liu T, Zhao L, Turng LS. Experiment and simulation of foaming injection molding of polypropylene/nano-calcium

- carbonate composites by supercritical carbon dioxide. Chin J Chem Eng. 2016;24(1):180-89. doi: 10.1016/j.cjche.2015.11.01.
- (15) Ghanbari A, Seyedin S, Nofar M. Mechanical properties and foaming behavior of polypropylene/elastomer/recycled carbon fiber composites. Polym Composite. 2021;42(7):3482–92. doi: 10.1002/pc.26073.
- (16) Zhou XX, Yu Y, Chen LH. Effects of zirconaluminate coupling agent on mechanical properties, rheological behavior and thermal stability of bamboo powder/polypropylene foaming composites. Eur Wood Wood Pro. 2015;73(2):199–7. doi: 10.1007/s00107-014-0853-1.
- (17) Cao L, Jiang T, Liu B. Effects of grafting and long-chain branching structures on rheological behavior, crystallization properties, foaming performance, and mechanical properties of polyamide 6. Epolys. 2022;22(1):249–63. doi: 10.1515/ epoly-2022-0030.
- (18) Luo D, Pei XL, Fu H, Yang X, Long S, Zhang L, et al. Modification of sodium bicarbonate and its effect on foaming behavior of polypropylene. Epoly. 2021;21(1):366–76. doi: 10.1515/epoly-2021-0032.
- (19) Simoncelli M, Marzari N, Cepellotti A. Generalization of Fourier's law into viscous heat equations. Phys Rev X. 2020;10(1):011019-130. doi: 10.1103/PhysRevX.10.011019.
- (20) Krause B, Rzeczkowski P, Pötschke P. Thermal conductivity and electrical resistivity of melt-mixed polypropylene composites containing mixtures of carbon-based fillers. Polym. 2019;11(6):1073-85. doi: 10.3390/polym11061073.
- (21) Riou M, Ausias G, Grohens Y. Thermoplastic foaming with thermo-expandable microcapsules: Mathematical modeling and numerical simulation for extrusion process. Chem Eng Sci. 2020;227:115852–67. doi: 10.1016/j.ces.2020.
- (22) Li Y, Yao Z, Chen Z, Cao K, Qiu SL, Zhu FJ, et al. Numerical simulation of polypropylene foaming process assisted by carbon dioxide: Bubble growth dynamics and stability. Chem

- Eng Sci. 2011;66(16):3656-65. doi: 10.1016/j.ces.2011. 04.035.
- (23) Ahmadi M, Rouhi S, Ansari R. Evaluating the thermal conductivity coefficient of polypropylene/graphene nanocomposites: A hierarchical investigation. J Mater. 2021;235(12):2762-70. doi: 10.1177/14644207211035415.
- (24) Barborik T, Zatloukal M. Effect of heat transfer coefficient, draw ratio, and die exit temperature on the production of flat polypropylene membranes. Phys Fluids. 2019;31(5):053101-24. doi: 10.1063/1.5094842.
- (25) Ma DD, Xia GD, Li YF, Jia YT, Wang J. Effects of structural parameters on fluid flow and heat transfer characteristics in microchannel with offset zigzag grooves in sidewall. Inter J Mass Tran. 2016;101:427–35. doi: 10.1016/j. ijheatmasstransfer.2016.04.091.
- (26) Li M, Li S, Liu B, Jiang T, Zhang D, Gong W. Rheological behavior, crystallization properties, and foaming performance of chain-extended poly (lactic acid) by functionalized epoxy. RSC Adv. 2021;11(52):32799-809. doi: 10.1039/d1ra06382k.
- (27) Gong W, Pei X, Yin X, Ban D, Fu H, He L. Synthesis of high-temperature thermally expandable microcapsules and their effects on foaming quality and surface quality of foamed ABS materials. Epoly. 2020;20(1):519–27. doi: 10.1016/j.jmrt.2021.05.077.
- (28) Deng R, Jiang T, Zhang C, Zeng X, Liu B, Yang J, et al. *In-situ* visualization of the cell formation process of foamed polypropylene under different foaming environments. Polym. 2021;13(9):1468–79. doi: 10.3390/poly13091468.
- (29) Llewelyn G, Rees A, Griffiths CA, Scholz SG. Advances in microcellular injection moulding. J Cell Plast. 2020;56(6):646-74. doi: 10.1177/0021955x20912207.
- (30) Liu Y, Zhu T, Bi J. Investigation on microstructures and mechanical properties of isotactic polypropylene parts fabricated by different process conditions with different aging periods. Polym. 2020;12(12):2828–38. doi: 10.3390/polym12122828.